Discrete rising tone elements of whistler-mode waves in the vicinity of the Moon: ARTEMIS observations

W. Sawaguchi[1], Y. Harada[1], S. Kurita[2]

[1]Department of Geophysics, Graduate School of Science, Kyoto University, Kyoto, Japan.
[2]Research Institute for Sustainable Humanosphere, Kyoto University, Uji, Japan.

Key Points:

- We present ARTEMIS observations of discrete rising-tone elements of whistler-mode waves in the vicinity of the Moon
- The observed frequency sweep rates are consistent with those predicted by a nonlinear growth theory of chorus emissions
- Our results imply that whistler-mode waves can grow nonlinearly into chorus-like emissions even around airless bodies without magnetospheres

Corresponding author: Wataru Sawaguchi, sawag@kugi.kyoto-u.ac.jp

Abstract

We report on discrete rising-tone elements of whistler-mode waves observed by Acceleration, Reconnection, Turbulence, and Electrodynamics of the Moon's Interaction with the Sun (ARTEMIS) in the vicinity of the Moon. The two-probe ARTEMIS observations suggest that a free energy source for the wave generation is provided by electron anisotropy resulting from lunar surface absorption and magnetic reflection. High time resolution dynamic spectra reveal that the waves consist of multiple rising tone elements, exhibiting striking similarities to the well-known whistler-mode chorus in planetary magnetospheres. The observed frequency sweep rates are generally consistent with those predicted by the nonlinear growth theory of chorus emissions by Omura et al. (2008). These results imply that whistler-mode waves can grow nonlinearly into chorus-like emissions even around airless bodies without magnetospheres and that a well-defined dipole field is not a prerequisite for the chorus generation.

Plain Language Summary

Whistler-mode chorus emission is a type of electromagnetic waves which sound like chirping of birds when converted into audio, because of the feature that its frequency rises or falls repeatedly in a second. Chorus is known to occur in planetary magnetospheres, and is important because it plays a role in formation of the hazardous radiation belts in the Earth's magnetosphere. Is it possible that chorus waves occur, for example, around the Moon? Although such an event has not been reported around airless bodies without magnetospheres like the Moon, whistler-mode waves, which can grow into chorus under certain conditions, are known to occur near the Moon. As there exist "seeds" of chorus, we decided to survey data obtained by spacecraft orbiting around the Moon, and we did find waves with chirping like chorus. In this paper, we investigate these chorus-like events in detail, and demonstrate that they are Moon-related waves, and that their chirping can be explained by the growth theory of chorus. These results provide a new insight into the lunar electromagnetic environment, which is getting important given the ongoing and planned exploration of the Moon, and also enable us to test the chorus theories with the exotic lunar conditions.

1 Introduction

Whistler-mode chorus emissions are narrow band emissions observed mainly in the inner magnetosphere of the Earth in a typical frequency range of 0.2 − 0.8 f_{ce}, where f_{ce} is the electron cyclotron frequency in the source region (Burtis & Helliwell, 1969, 1976; Tsurutani & Smith, 1974). When converted to audio, their frequent repetition of rising or falling tones results in sounds that resemble chirping of birds, hence the name. Chorus emissions have been extensively investigated because they potentially play an important role in the formation and dynamics of the Earth's outer radiation belt (Horne et al., 2005; Thorne et al., 2013). In addition to the terrestrial magnetosphere, they have been found in the Jovian (Coroniti et al., 1980; Scarf et al., 1981; Menietti, Horne, et al., 2008), Saturnian (Hospodarsky et al., 2008; Menietti, Santolik, et al., 2008) and Martian (Harada et al., 2016) magnetospheres, but they have not yet been found around airless bodies without magnetospheres.

The generation of whistler-mode waves is explained by the linear theory (Tsurutani et al., 1979), in which the free energy of waves is provided by a temperature anisotropy (higher perpendicular temperature than parallel temperature) of electrons injected from Earth's magnetotail (Kennel & Petschek, 1966; Li et al., 2010). However, the linear theory cannot explain the characteristic chirping of chorus emissions. Thus, nonlinear growth theories have attracted great attention. When a whistler-mode wave occurs by cyclotron resonance with electrons, some of the resonant electrons can be trapped in the wave field (Dysthe, 1971), forming an electron 'hole' in the wave phase space. This hole can form a resonant current, which then causes nonlinear growth of a wave with a rising frequency (Nunn, 1974; Omura et al., 1991). By introducing inhomogeneity ratio S and analytically calculating S which maximizes the resonant current, Omura et al. (2008) predicted the sweep rate of rising tone elements of chorus emissions. This theory successfully predicts observed sweep rates of chorus elements (Cully et al., 2011; Kurita et al., 2012).

Although the Moon does not have a global, intrinsic magnetic field and a dense atmosphere, interaction of plasmas in the solar wind and in the Earth's magnetotail with the lunar surface and crustal magnetic fields causes a variety of complex, time-varying plasma phenomena (Halekas et al., 2011; Nakagawa, 2016; Harada & Halekas, 2016). Among them, it is known that whistler-mode waves can be excited in the vicinity of the Moon as a result of cyclotron resonance of waves traveling toward the Moon with upward-traveling electrons magnetically mirrored by lunar crustal magnetic fields (Halekas, Poppe, Delory, et al., 2012; Halekas, Poppe, Farrell, et al., 2012; Harada et al., 2014, 2015). A free energy source for the wave excitation is provided by effective temperature anisotropy in electron velocity distribution functions resulting from the surface absorption of parallel electrons and magnetic reflection of perpendicular electrons. As these whistler-mode waves around the Moon can have as large amplitudes as those in the Earth's magnetosphere, one might expect that they could grow nonlinearly in a manner similar to chorus emissions.

In this paper, we report on the existence of discrete rising-tone elements of whistler-mode waves observed by the Acceleration, Reconnection, Turbulence, and Electrodynamics of the Moon's Interaction with the Sun (ARTEMIS) mission (Angelopoulos, 2011) in the vicinity of the Moon along with results of two ways of analysis: two-point observations and data-theory comparison. To check if they are related to the Moon, we compare wave spectra and electron pitch angle distributions observed by one probe magnetically connected to the Moon with those observed by the other unconnected probe. These two-point observations demonstrate that the observed whistler-mode waves are indeed moon-related as suggested by the previous studies. Furthermore, we compare the frequency sweep profiles of the observed rising tone elements with those predicted by the nonlinear growth theory of chorus emissions by Omura et al. (2008). Based on the theory, relationship between sweep rates and wave amplitudes can be estimated from the observed electron distributions, magnetic field strength, and electron density. The predictions show a good agreement with the observations. These results imply that Moon-related whistler-mode waves can grow nonlinearly into chorus-like emissions.

2 Observations

First we present overviews of two cases on ARTEMIS observations of rising tone elements of whistler-mode waves around the Moon. We use field and plasma data obtained by the search coil magnetometer (SCM) (Roux et al., 2008), flux gate magnetometer (FGM) (Auster et al., 2008), and electrostatic analyzer (ESA) (McFadden et al., 2008) instruments on board ARTEMIS.

Figure 1 shows an event with multiple discrete rising tone elements observed by ARTEMIS P2 on 10 September 2011. During this time interval, the Moon was located in the terrestrial magnetotail (Figure 1a), and ARTEMIS P1 and P2 were located on the dayside and nightside of the Moon, respectively as shown in the insert of Figure 1a. The hot electrons detected by P1 (Figure 1e) and by P2 (Figure 1i) indicate that the Moon was located in the Earth's plasma sheet. Clear flux depletions are seen intermittently during 05:37:50-05:38:47 UT for parallel electrons in P2 pitch angle distributions (Figure 1j). Taken together with the spacecraft position and magnetic field direction (Figures 1a and 1h), this indicate that P2 was connected by a magnetic field line to the Moon and that loss cones are formed in the upward-traveling electron distributions by the combination of surface absorption and reflection by crustal magnetic fields (Halekas, Poppe, Farrell, et al., 2012). Concurrently with the loss cone observations, SCM detected electromagnetic waves just below $0.5f_{ce}$ (Figure 1k), suggesting that the effective temperature anisotropy resulting from the electron loss cone distributions drives whistler-mode waves as proposed by the previous studies (Halekas, Poppe, Farrell, et al., 2012; Harada et al., 2014, 2015). Meanwhile, P1 observed nearly isotropic electron distributions (Figure 1f) and no waves just below $0.5f_{ce}$ (Figure 1g) during 05:38-05:39 UT. This suggests that P1 was magnetically unconnected to the Moon at this time and that the waves detected by P2 are of Moon-related origin.

To resolve short timescale features such as rapid and repetitive rising tone elements possibly present in the wave fields, we utilize SCM waveform data (available for limited time segments). Figures 1b–1d show dynamic spectra generated from SCM waveform data obtained by P2 of wave power, wave normal angle, and ellipticity, respectively. The wave normal angle and ellipticity are computed by the method of singular value decomposition (SVD) of the complex spectral matrix (Santolik et al., 2003; Taubenschuss & Santolik, 2019). We identify discrete rising tone elements as denoted by the magenta arrows with each element rapidly sweeping in frequency within a second (Figure 1b). These spectral features are reminiscent of the whistler-mode chorus emissions observed in the Earth's inner magnetosphere (Burtis & Helliwell, 1969, 1976; Tsurutani & Smith, 1974). Furthermore, right-handed polarization (Figure 1d) of the detected waves below f_{ce} is consistent with the whistler-mode, and the relatively small wave normal angles (Figure 1c) is consistent with the cold plasma theory (Kennel & Petschek, 1966).

Figure 2 shows another case. The Moon-related particle and wave signatures during this event were first investigated in detail by Halekas, Poppe, Farrell, et al. (2012), though they do not mention the rising tone features discussed in this paper. As is the case for the event shown in Figure 1, the Moon and P1 were located in the magnetotail plasma sheet (Figures 2e and 2i), while P2 was located distant from the Moon and observed slightly different electron characteristics after 12:09:30 UT (Figures 2a and 2e). As noted by Halekas, Poppe, Farrell, et al. (2012), the P1 data show clear loss cone signatures (Figure 2j) and wave power near $0.5f_{ce}$ (Figure 2k). Meanwhile, the P2 data show no evidence for similar signatures (Figures 2f and 2g). The dynamic spectra generated from SCM waveform data (Figures 2b–2d) demonstrate the presence of multiple rising tone elements and wave properties consistent with the whistler-mode. Aside from demonstrating that the rising tone event shown in Figure 1 is not a lone case, the event shown in Figure 2 is particularly noteworthy because the rising tone elements have frequencies sweeping across $0.5f_{ce}$ without a gap at $0.5f_{ce}$. Such "no-gap" whistler mode waves are not the most common type in the Earth's inner magnetosphere and show characteristic spatial distributions (Teng et al., 2019).

3 Comparison with Theoretical Prediction

According to the nonlinear wave growth theory developed by Omura et al. (2008), by assuming a delta function for the velocity distribution function of resonant electrons at $v_\perp = V_{\perp 0}$, the sweep rate of the chorus emission can be approximated as

$$\frac{\partial \omega}{\partial t} = \frac{0.4\delta}{\gamma\xi}\frac{V_{\perp 0}}{c}\frac{\omega}{\Omega_e}\left(1-\frac{V_R}{V_g}\right)^{-2}\frac{B_w}{B_0}\Omega_e^2 \quad (1)$$

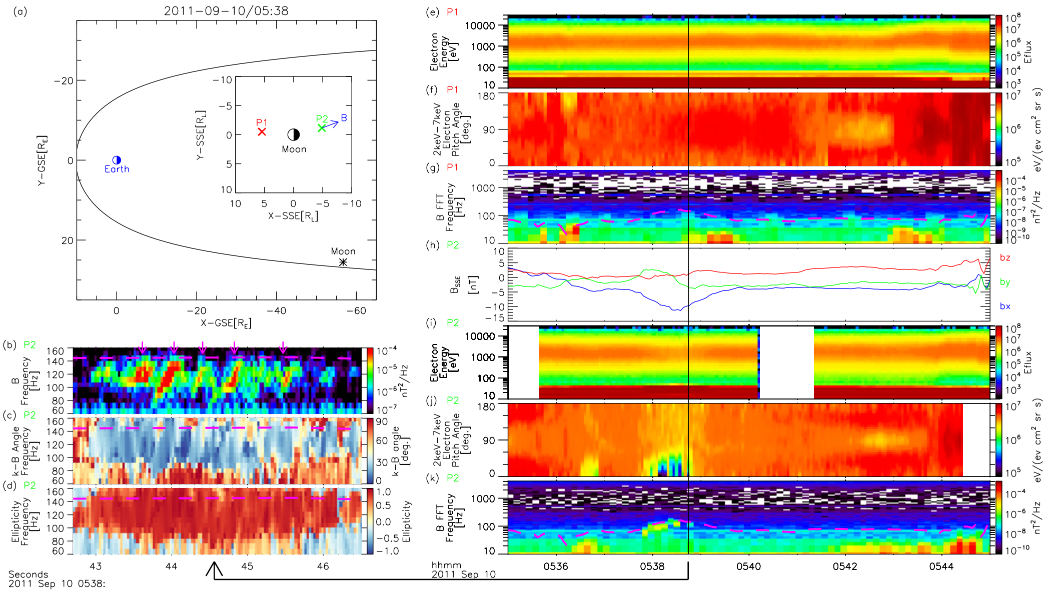

Figure 1. Overview of ARTEMIS observations of rising tone elements of whistler-mode waves on 10 September 2011. (a) The position of the Moon in the geocentric solar ecliptic (GSE) coordinate system, where the blue circle, the black asterisk, and the black line represent the Earth, the Moon and a typical magnetopause location (Shue et al., 1997), respectively. The insert shows the positions of the probes in the selenocentric solar ecliptic (SSE) coordinate system, where the black circle, and red and green X-marks, and blue arrow represent the Moon, P1 and P2, and magnetic field direction, respectively; Dynamic spectra generated from SCM waveform data obtained by ARTEMIS P2 at 05:38:42.7–05:38:46.5 of (b) wave spectral density (rising tone elements are denoted by the magenta arrows), (c) wave normal angle with respect to the background magnetic field, and (d) ellipticity (+1: right-handed circular polarization; −1: left-handed circular polarization) with respect to the background magnetic field. Time series data from ARTEMIS P1 and P2 at 05:35–05:45 UT of (e, i) energy spectra of electrons in units of differential energy flux (labeled "Eflux" for short, eV/cm^2/sr/s/eV), (f, j) pitch angle spectra of 2–7 keV electrons in units of differential energy flux, (g, k) onboard FFT magnetic wave spectra, (h) magnetic fields in the SSE coordinate system. The data shown in Figures 1e–1g and 1h–1k are obtained by P1 and P2, respectively. The dashed magenta lines in Figures 1b–1d, 1g and 1k represent half the electron cyclotron frequency.

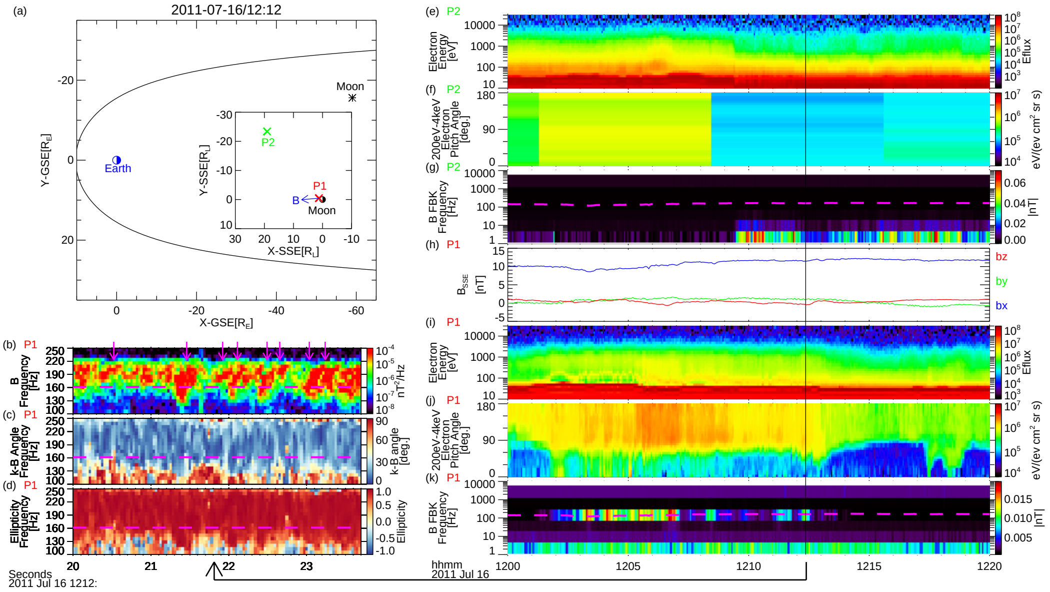

Figure 2. Overview of ARTEMIS observations of rising tone elements of whistler-mode waves on 11 July 2011 in the same format as Figure 1 except that Figures 2b–d and Figures 2h–k are generated from P1 data, and Figures 2e–g are from P2, and that Figures 2g and k are generated from the filter bank data.

with

$$\delta^2 = 1 - \frac{\omega^2}{c^2k^2}, \tag{2}$$

$$\xi^2 = \frac{\omega(\Omega_e - \omega)}{\omega_{pe}^2}, \tag{3}$$

$$\gamma = \sqrt{1 - \frac{v_\parallel^2 + v_\perp^2}{c^2}}, \tag{4}$$

$$V_R = \frac{1}{k}\left(\omega - \frac{\Omega_e}{\gamma}\right), \tag{5}$$

and

$$V_g = \frac{c\xi}{\delta}\left[\xi^2 + \frac{\Omega_e}{2(\Omega_e - \omega)}\right]^{-1}. \tag{6}$$

Here, $\Omega_e = eB_0/m_e$ is the electron cyclotron frequency in the source region, $\omega_{pe} = \sqrt{n_e e^2/\epsilon_0 m_e}$ is the electron plasma frequency, n_e, e, and m_e are the number density, charge, and mass of the electrons, ϵ_0 is the permittivity in a free space, B_0 is the background magnetic field intensity, $v_\parallel = V_R$ and $v_\perp = V_{\perp 0}$ are the parallel and perpendicular velocity, and k, ω, and B_w are the wave number, frequency, and amplitude of the wave. Actual electron velocity distributions may differ from the assumed ring distribution, but Cully et al. (2011) showed that equation (1) provides a good estimate by choosing $V_{\perp 0}$ as the perpendicular velocity above which the velocity distribution function of resonant electrons becomes isotropic and below which the distribution is anisotropic.

To compare the observed elements with equation (1), we first estimate $V_{\perp 0}$ from particle data. Figure 3a shows the observed electron velocity distribution function. The magenta lines show the resonant ellipses for the lower and upper wave frequencies (0.2–0.45 f_{ce}) assuming cyclotron resonance of parallel (upward) electrons

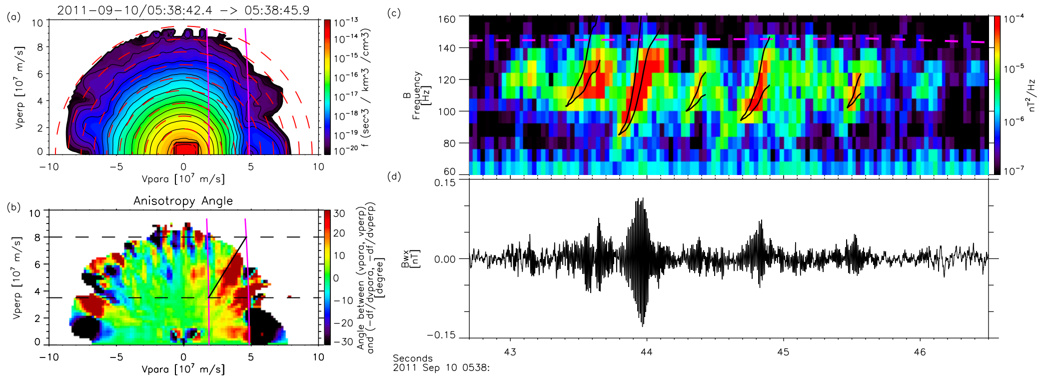

Figure 3. Comparison of the observed electron distributions and waves with theoretical prediction for the event shown in Figure 1: (a) electron distribution function $f(v_\parallel, v_\perp)$ with resonant ellipses for the upper and lower wave frequencies (magenta lines) and isotropic circles (red dashed circles) for reference, (b) anisotropy of the electron distribution function calculated as the angle of the gradient of the distribution function from the radial direction, (c) wave dynamic spectra with half the electron cyclotron frequency (magenta dahed line) and theoretically predicted sweeps (black lines), and (d) waveform of a magnetic field component perpendicular to the background magnetic field.

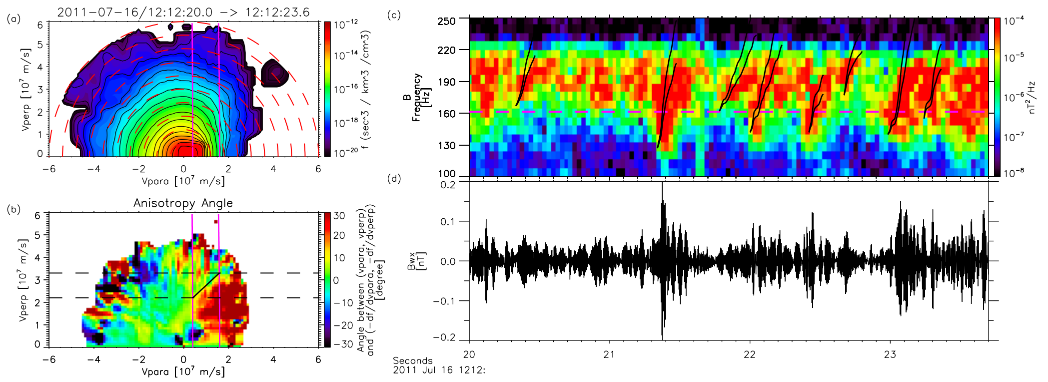

Figure 4. Comparison of the observed electron distributions and waves with theoretical prediction for the event shown in Figure 2 in the same format as Figure 3.

with anti-parallel (downward) propagating waves. It is seen that the electron distribution function is highly deformed from isotropic between these resonant ellipses, suggesting that these anisotropic electrons can provide a source of free energy for the whistler-mode waves. To further investigate which portion of the distribution function can contribute to the wave growth, we visualize the local anisotropy of electron distribution function in Figure 3b by calculating the angle between the radial direction in the velocity space and the gradient of the distribution function at each point, namely computing

$$\theta_A = \tan^{-1}\left(\frac{\partial f}{\partial v_\parallel}\bigg/\frac{\partial f}{\partial v_\perp}\right) - \tan^{-1}\left(\frac{v_\parallel}{v_\perp}\right). \tag{7}$$

The polarity of the angle is chosen such that a positive angle corresponds to whistler-unstable anisotropy (effectively higher perpendicular temperature compared to the parallel temperature) in $v_\parallel > 0$. It is seen that the loss cone corresponds to large positive angles as shown in red colors in Figure 3b. In Figure 3b, we draw a black line so that the velocity distribution function is nearly isotropic above the black line and anisotropic below it. Based on the Cully et al. (2011)'s results, we choose $V_{\perp 0} \sim 3.5 \times 10^7$ and 8×10^7 m/s as lower and upper bound estimates for this event. Next, we apply a high-pass filter to the waveform magnetic field data of SCM to reduce low-frequency noise, and then rotate them into the magnetic field aligned coordinates based on the FGM background field data. For the instantaneous amplitudes B_w, we use the absolute values of local maxima or minima of the perpendicular components of the waveform data (Figure 3d). The instantaneous frequencies ω are then estimated from the intervals of two zero-crossings just beside each maximum or minimum. Finally, we substitute the values of $V_{\perp 0}$, B_w, and ω to the equation (1) and draw the growth prediction lines (one from the estimated minimum $V_{\perp 0}$ and the other from the maximum $V_{\perp 0}$) over the wave dynamic spectra in Figure 3c with the initial frequency and time duration of each element chosen by hand. We can see that the prediction lines roughly follow the observed frequency sweep of each element, demonstrating that the observed rising tones are consistent with the nonlinear growth theory of chorus emissions.

We perform a similar analysis for the event shown in Figure 2. Figure 4 shows the results of the analysis. Here we estimate the wave frequencies as 0.38–0.7 f_{ce}. We observe a highly deformed distribution function between the resonant ellipses (Figure 4a), and we choose 2.2×10^7 and 3.3×10^7 m/s as the lower and upper bound estimates of $V_{\perp 0}$ (Figure 4b). Although the comparison is not as straightforward as the former case because of the overlapped elements, the theoretically predicted sweep profiles show a general agreement with the observed ones (Figure 4c), again demonstrating the consistency between the observation and theory.

4 Conclusions and Implications

We presented case studies of whistler-mode waves with rising tone elements observed by ARTEMIS in the vicinity of the Moon. The results show that Moon-related whistler-mode waves, which are driven by electron anisotropy resulting from the lunar surface absorption and magnetic reflection, can grow nonlinearly and develop discrete rising tone elements as predicted by Omura et al. (2008) theory. To our knowledge, this is the first report on whistler-mode emissions with chorus-like rising tone elements observed around airless bodies without magnetospheres. The presence of chorus-like emissions around the Moon implies that an intrinsic dipole magnetic field may not be a necessary condition for the chorus generation. One event shows rising tone elements with frequencies sweeping across $0.5f_{ce}$ without a gap at $0.5f_{ce}$, which could have implications for generation mechanisms of the gap at $0.5f_{ce}$ typically seen for the whistler-mode chorus. We plan to conduct follow-up studies on statistical properties of the Moon-related whistler-mode waves, thereby further characterizing their similarities to, and differences from, the chorus emissions in the Earth's inner magnetosphere. The investigation of Moon-related whistler-mode waves would not only contribute to our understanding of the time-variable lunar electromagnetic environment, but also provide an important test case for theories of generation and development of the whistler-mode chorus emissions.

Acknowledgments

We acknowledge NASA contract NAS5-02099 and V. Angelopoulos for use of data from the THEMIS Mission. Specifically: C. W. Carlson and J. P. McFadden for use of ESA data, O. LeContel and the late A. Roux for use of SCM data, and K. H. Glassmeier, U. Auster and W. Baumjohann for the use of FGM data provided under the lead of the Technical University of Braunschweig and with financial support through the German Ministry for Economy and Technology and the German Center for Aviation and Space (DLR) under contract 50 OC 0302. ARTEMIS data are publicly available at http://artemis.ssl.berkeley.edu. We would like to thank C. M. Cully for helpful comments.

References

Angelopoulos, V. (2011, DEC). The ARTEMIS mission. In (Vol. 165, p. 3-25). doi: 10.1007/s11214-010-9687-2

Auster, H. U., Glassmeier, K. H., Magnes, W., Aydogar, O., Baumjohann, W., Constantinescu, D., . . . Wiedemann, M. (2008, DEC). The THEMIS Fluxgate Magnetometer. *SPACE SCIENCE REVIEWS*, *141*(1-4), 235-264. doi: 10.1007/s11214-008-9365-9

Burtis, W. J., & Helliwell, R. A. (1969). Banded chorus – A new type of VLF radiation observed in the magnetosphere by OGO 1 and OGO 3. *Journal of Geophysical Research*, *74*(11), 3002–3010. doi: 10.1029/JA074i011p03002

Burtis, W. J., & Helliwell, R. A. (1976). Magnetospheric chorus: Occurrence patterns and normalized frequency. *Planetary and Space Science*, *24*(11), 1007–1024. doi: 10.1016/0032-0633(76)90119-7

Coroniti, F. V., Scarf, F. L., Kennel, C. F., Kurth, W. S., & Gurnett, D. A. (1980). Detection of Jovian whistler mode chorus; Implications for the Io torus aurora. *Geophysical Research Letters*, *7*(1), 45–48. doi: 10.1029/GL007i001p00045

Cully, C. M., Angelopoulos, V., Auster, U., Bonnell, J., & Le Contel, O. (2011). Observational evidence of the generation mechanism for rising-tone chorus. *Geophysical Research Letters*, *38*(1). doi: 10.1029/2010GL045793

Dysthe, K. B. (1971). Some studies of triggered whistler emissions. *Journal of Geophysical research*, *76*(28), 6915–6931. doi: 10.1029/JA076i028p06915

Halekas, J. S., Poppe, A., Delory, G. T., Farrell, W. M., & Horányi, M. (2012). Solar wind electron interaction with the dayside lunar surface and crustal magnetic fields: Evidence for precursor effects. *Earth, planets and space*, *64*(2), 3. doi: 10.5047/eps.2011.03.008

Halekas, J. S., Poppe, A. R., Farrell, W. M., Delory, G. T., Angelopoulos, V., McFadden, J. P., . . . others (2012). Lunar precursor effects in the solar wind and terrestrial magnetosphere. *Journal of Geophysical Research: Space Physics*, *117*(A5). doi: 10.1029/2011JA017289

Halekas, J. S., Saito, Y., Delory, G. T., & Farrell, W. M. (2011). New views of the lunar plasma environment. *Planetary and Space Science*, *59*(14), 1681–1694. doi: 10.1016/j.pss.2010.08.011

Harada, Y., Andersson, L., Fowler, C. M., Mitchell, D. L., Halekas, J. S., Mazelle, C., . . . others (2016). MAVEN observations of electron-induced whistler mode waves in the Martian magnetosphere. *Journal of Geophysical Research: Space Physics*, *121*(10), 9717–9731. doi: 10.1002/2015GL067040

Harada, Y., & Halekas, J. S. (2016). Upstream Waves and Particles at the Moon. In Keiling, A and Lee, DH and Nakariakov, V (Ed.), *LOW-FREQUENCY WAVES IN SPACE PLASMAS* (Vol. 216, p. 307-322).

Harada, Y., Halekas, J. S., Poppe, A. R., Kurita, S., & McFadden, J. P. (2014). Extended lunar precursor regions: Electron-wave interaction. *Journal of Geophysical Research: Space Physics*, *119*(11), 9160–9173. doi: 10.1002/2014JA020618

Harada, Y., Halekas, J. S., Poppe, A. R., Tsugawa, Y., Kurita, S., & McFadden, J. P. (2015, JUN). Statistical characterization of the foremoon particle and wave morphology: ARTEMIS observations. *JOURNAL OF GEOPHYSICAL RESEARCH-SPACE PHYSICS*, *120*(6), 4907-4921. doi: 10.1002/2015JA021211

Horne, R. B., Thorne, R. M., Shprits, Y. Y., Meredith, N. P., Glauert, S. A., Smith, A. J., ... Decreau, P. M. E. (2005, SEP 8). Wave acceleration of electrons in the Van Allen radiation belts. *NATURE*, *437*(7056), 227-230. doi: 10.1038/nature03939

Hospodarsky, G. B., Averkamp, T. F., Kurth, W. S., Gurnett, D. A., Menietti, J. D., Santolik, O., & Dougherty, M. K. (2008). Observations of chorus at Saturn using the Cassini Radio and Plasma Wave Science instrument. *Journal of Geophysical Research: Space Physics*, *113*(A12). doi: 10.1029/2008JA013237

Kennel, C. F., & Petschek, H. E. (1966). Limit on stably trapped particle fluxes. *Journal of Geophysical Research*, *71*(1), 1–28. doi: 10.1029/JZ071i001p00001

Kurita, S., Katoh, Y., Omura, Y., Angelopoulos, V., Cully, C. M., Le Contel, O., & Misawa, H. (2012). THEMIS observation of chorus elements without a gap at half the gyrofrequency. *Journal of Geophysical Research: Space Physics*, *117*(A11). doi: 10.1029/2012JA018076

Li, W., Thorne, R. M., Nishimura, Y., Bortnik, J., Angelopoulos, V., McFadden, J. P., ... Auster, U. (2010, JUN 8). THEMIS analysis of observed equatorial electron distributions responsible for the chorus excitation. *JOURNAL OF GEOPHYSICAL RESEARCH-SPACE PHYSICS*, *115*. doi: 10.1029/2009JA014845

McFadden, J. P., Carlson, C. W., Larson, D., Ludlam, M., Abiad, R., Elliott, B., ... Angelopoulos, V. (2008, DEC). The THEMIS ESA Plasma Instrument and In-flight Calibration. *SPACE SCIENCE REVIEWS*, *141*(1-4), 277-302. doi: 10.1007/s11214-008-9440-2

Menietti, J. D., Horne, R. B., Gurnett, D. A., Hospodarsky, G. B., Piker, C. W., & Groene, J. B. (2008). A survey of Galileo plasma wave instrument observations of Jovian whistler-mode chorus. *Annales Geophysicae*, *26*(7), 1819–1828. Retrieved from `https://www.ann-geophys.net/26/1819/2008/` doi: 10.5194/angeo-26-1819-2008

Menietti, J. D., Santolik, O., Rymer, A. M., Hospodarsky, G. B., Gurnett, D. A., & Coates, A. J. (2008). Analysis of plasma waves observed in the inner Saturn magnetosphere. In *Annales geophysicae: atmospheres, hydrospheres and space sciences* (Vol. 26, p. 2631). doi: 10.1029/2007JA012856

Nakagawa, T. (2016). ULF/ELF Waves in Near-Moon Space. In Keiling, A and Lee, DH and Nakariakov, V (Ed.), *LOW-FREQUENCY WAVES IN SPACE PLASMAS* (Vol. 216, p. 295-306).

Nunn, D. (1974). A self-consistent theory of triggered VLF emissions. *Planetary and Space Science*, *22*(3), 349–378. doi: 10.1016/0032-0633(74)90070-1

Omura, Y., Katoh, Y., & Summers, D. (2008). Theory and simulation of the generation of whistler-mode chorus. *Journal of Geophysical Research: Space Physics*, *113*(A4). doi: 10.1029/2007JA012622

Omura, Y., Nunn, D., Matsumoto, H., & Rycroft, M. J. (1991). A review of observational, theoretical and numerical studies of VLF triggered emissions. *Journal of Atmospheric and Terrestrial Physics*, *53*(5), 351–368. doi: 10.1016/

0021-9169(91)90031-2

Roux, A., Le Contel, O., Coillot, C., Bouabdellah, A., de la Porte, B., Alison, D., . . . Vassal, M. C. (2008, DEC). The Search Coil Magnetometer for THEMIS. *SPACE SCIENCE REVIEWS*, *141*(1-4), 265-275. doi: 10.1007/s11214-008-9455-8

Santolik, O., Parrot, M., & Lefeuvre, F. (2003, FEB 12). Singular value decomposition methods for wave propagation analysis. *RADIO SCIENCE*, *38*(1). doi: {10.1029/2000RS002523}

Scarf, F. L., Gurnett, D. A., & Kurth, W. S. (1981). Measurements of plasma wave spectra in Jupiter's magnetosphere. *Journal of Geophysical Research: Space Physics*, *86*(A10), 8181-8198. Retrieved from `https://agupubs.onlinelibrary.wiley.com/doi/abs/10.1029/JA086iA10p08181` doi: 10.1029/JA086iA10p08181

Shue, J. H., Chao, J. K., Fu, H. C., Russell, C. T., Song, P., Khurana, K. K., & Singer, H. J. (1997, MAY 1). A new functional form to study the solar wind control of the magnetopause size and shape. *JOURNAL OF GEOPHYSICAL RESEARCH-SPACE PHYSICS*, *102*(A5), 9497-9511. doi: 10.1029/97JA00196

Taubenschuss, U., & Santolik, O. (2019, JAN). Wave Polarization Analyzed by Singular Value Decomposition of the Spectral Matrix in the Presence of Noise. *SURVEYS IN GEOPHYSICS*, *40*(1), 39-69. doi: {10.1007/s10712-018-9496-9}

Teng, S., Tao, X., & Li, W. (2019, APR 16). Typical Characteristics of Whistler Mode Waves Categorized by Their Spectral Properties Using Van Allen Probes Observations. *GEOPHYSICAL RESEARCH LETTERS*, *46*(7), 3607-3614. doi: {10.1029/2019GL082161}

Thorne, R. M., Li, W., Ni, B., Ma, Q., Bortnik, J., Chen, L., . . . Kanekal, S. G. (2013, DEC 19). Rapid local acceleration of relativistic radiation-belt electrons by magnetospheric chorus. *NATURE*, *504*(7480), 411+. doi: 10.1038/nature12889

Tsurutani, B. T., & Smith, E. J. (1974). Postmidnight chorus: A substorm phenomenon. *Journal of Geophysical Research*, *79*(1), 118–127. doi: 10.1029/JA079i001p00118

Tsurutani, B. T., Smith, E. J., West, H. I., & Buck, R. M. (1979). Chorus, energetic electrons and magnetospheric substorms. In *Wave Instabilities in Space Plasmas* (pp. 55–62). Springer.